Fault Detection of Helicopter Gearboxes Using the Multi-Valued Influence Matrix Method

H. Chin
Graduate Research Assistant[1].

K. Danai
Associate Professor.
Mem. ASME

Department of Mechanical Engineering,
University of Massachusetts,
Amherst, MA 01003

D. G. Lewicki
U.S. Army Research Laboratory,
Vehicle Propulsion Directorate,
NASA Lewis Research Center,
Cleveland, OH 44135

Fault detection of a helicopter gearbox by pattern classification is discussed. The detection system is composed of two components, a quantization matrix *to flag the measurements, and a* multi-valued influence matrix *(MVIM) that represents the behavior of measurements during normal operation and at fault instances. Both the* quantization matrix *and the* influence matrix *are tuned during a training session so as to minimize the error in detection. This detection system was applied to vibration measurements collected from a helicopter gearbox test stand during accelerated fatigue tests and at various fault instances. The results indicate that the MVIM method provides accurate detection when the full range of faults effects on the measurements are included in the training set. Furthermore, the fixed structure of MVIM allows evaluation of individual measurements. This feature was utilized to select a subset of measurements crucial to detection.*

1 Introduction

Helicopter drive trains are significant contributors to both maintenance cost and flight safety incidents. Drive trains comprise almost 30 percent of maintenance costs and 16 percent of mechanically related malfunctions that often result in the loss of aircraft (Chin and Danai, 1991). Future helicopters like the COMANCHE and fixed wing aircraft like the ATF require increased levels of mission capability that simply cannot be met without advancing the state of the art in detection, particularly in critical components like the drive trains. These detection systems should be reliable so as to avoid unnecessary emergency landings due to false alarms, and should be fast to be applicable on-line.

For fault detection of helicopter drive trains, either debris sensors (chip detectors) are used to detect the presence of residues caused by component failures (Collier-March and Astridge, 1985), or vibration analysis is employed to identify the presence of any abnormalities that may have been resulted from a fault (e.g., Braun, 1986; Kaufman, 1975). Although chip detectors are effective in detecting failures which produce debris, they are not completely reliable due to their insensitivity to wear-related faults. Vibration analysis, on the other hand, is believed to provide a more generic basis for fault detection (e.g., Cempel, 1988; Astridge, 1986). As such, considerable effort has been directed toward the identification of features of vibration that are affected by specific faults (e.g., Pratt, 1986; Mertaugh, 1986) and the development of signal processing techniques that can quantify such features through various parameters (Dimarogonas and Haddad, 1992). For example, the crest factor of vibration, which represents the peak-to-rms ratio of vibration, has been shown to increase when localized faults such as tooth cracks occur (Braun, 1986). For detection purposes, the parameter values (measurements) obtained through signal processing are analyzed for any abnormalities, and flagged once such abnormality is observed. The simplest and most common method of flagging is applying thresholds to these parameters.

The fundamental problem with the current method of fault detection is that it is at the mercy of the flagging operation. Flags can be posted due to noise, causing false alarms, or the effect of faults may not be identified through flagging, so faults may remain undetected. Neither false alarms nor undetected faults are acceptable for helicopter fault detection, since false alarms result in unnecessary emergency landings, and undetected faults may cause catastrophic failures.

In order to cope with the uncertainty of flagged measurements, pattern classification techniques can be employed. Among the various pattern classifiers used for detection, artificial neural nets are the most notable due to their nonparametric nature (independence of the probabilistic structure of the vibration data), and their ability to generate complex decision regions. However, neural nets generally require extensive training to develop the decision regions (detection model). In cases such as helicopter drive trains, where adequate data is usually not available for training,

[1]Presently with Technology Integration Inc., Bedford, MA.

Contributed by the Power Transmission and Gear Committee for publication in the JOURNAL OF MECHANICAL DESIGN. Manuscript received May 1992; revised Jan. 1995. Associate Technical Editor: D. R. Houser.

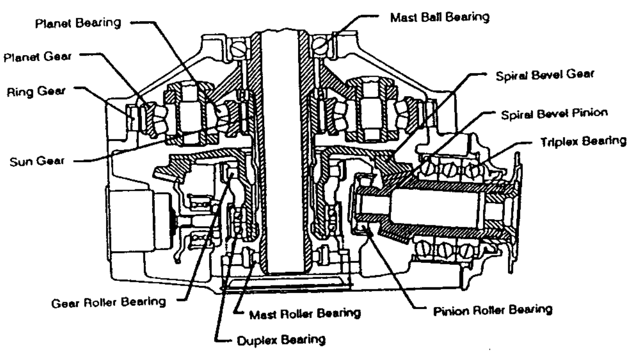

Fig. 1 Configuration of the OH-58A main rotor transmission

artificial neural nets may produce false alarms or leave faults undetected.

In this paper, fault detection of helicopter gearboxes by the Multi-Valued Influence Matrix (MVIM) method (Danai and Chin, 1991) is investigated. The MVIM method uses nonparametric pattern classification to estimate its detection model, so like artificial neural nets is independent of the probabilistic structure of the vibration data. However, this method benefits from an efficient learning algorithm based on detection error feedback that allows it to estimate its detection model based on a small number of measurement-fault data. The MVIM method can also assess the significance of individual measurements in detection based on their influence on the speed of training of the system.

To train and test the MVIM, vibration data reflecting the effect of various helicopter main rotor transmission faults were collected at NASA. This vibration data were then processed through a micro-computer customized for vibration signal processing to obtain parameters which represented various features of the gearbox vibration. The obtained parameters were then utilized to train the MVIM method and test its performance. Detection results indicate that the MVIM method produced accurate detection when trained with the full range of fault effects on the parameters, and that it produced better overall detection than a feedforward neural net trained with backpropagation learning. The MVIM method was also utilized to rank the parameters for their significance in detection. It is shown that through this ranking procedure the optimal subset of parameters for detection can be obtained, which is important in reducing processing time for in-flight detection of helicopter gearboxes.

2 Experimental

Vibration data were collected at the NASA Lewis Research Center as part of a joint NASA/Navy/Army Advanced Lubricants Program. Various component failures in an OH-58A main rotor transmission were produced during experiments (Lewicki et al., 1992). The configuration of the transmission which was tested in the NASA 500-hp Helicopter Transmission Test Stand is shown in Fig. 1. The vibration signals were recorded from eight piezoelectric accelerometers (frequency range of up to 10 KHz) using an FM tape recorder. The signals were recorded once every hour, for about one to two minutes per recording (at the tape speed of 30 in/sec, providing a bandwidth of 20 KHz). Two magnetic chip detectors were also used to detect the debris caused by component failures. The location and orientation of the accelerometers are shown in Fig. 2.

In these experiments accelerated fatigue tests were performed. The transmission was run under a constant load and was disassembled and inspected periodically or when one of the chip detectors indicated a failure. A total of five tests were performed, where each test was run between nine to fifteen days for approximately four to eight hours a day. New components were used at the start of each test. When a component fault was detected during a test, it was replaced with a new one for the remainder of the test. Among the eleven failures which occurred during these tests (see Table 1), there were three cases of planet bearing failure, three cases of sun gear failure, two cases of top housing cover cracking, and one case each of spiral bevel pinion, mast bearing, and planet gear failure. Insofar as fault detection during these tests, the chip detectors were reliable in detecting failures in which a significant amount of debris was generated, such as the planet bearing failures and one sun gear failure. The remaining failures were detected during routine disassembly and inspection.

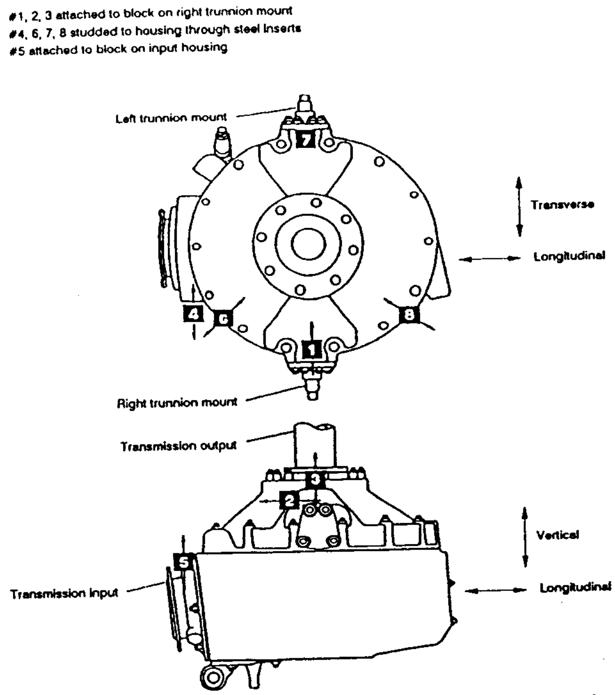

Fig. 2 Location of the accelerometers on the test stand

Table 1 Faults encountered during the experiments

Test #	Number of Days	Failures
1	9	Sun gear tooth pit Spiral bevel pinion scoring/heavy wear
2	9	None
3	13	Planet bearing #2 inner race spall Top cover housing crack Planet bearing #2 inner race spall Micropitting on mast bearing
4	15	Planet bearing #3 inner race spall Sun gear tooth pit
5	11	Sun gear teeth spalls Planet gear tooth spall Top housing cover crack

3 Signal Processing

In order to identify the effect of faults on the vibration data, the vibration signals obtained from the five tests were digitized and processed by a commercially available diagnostic analyzer (Stewart Hughes Limited, 1986). Three processing modules of the analyzer were used: (*1*) *Statistical Analysis* (*STAT*), (*2*) *Baseband Power Spectrum Analysis* (*BBPS*), and (*3*) *Bearing Analysis* (*BRGA*). The fourth module of the diagnostic analyzer provides synchronous time averaged parameters for individual gears, which are expected to be crucial for gear failure diagnosis. The parameters from this

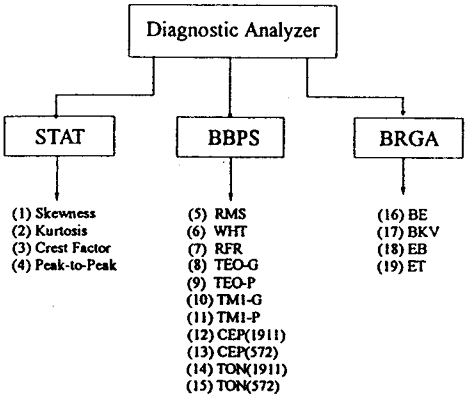

Fig. 3 Parameters obtained from the diagnostic analyzer (Stewart Hughes Limited, 1986)

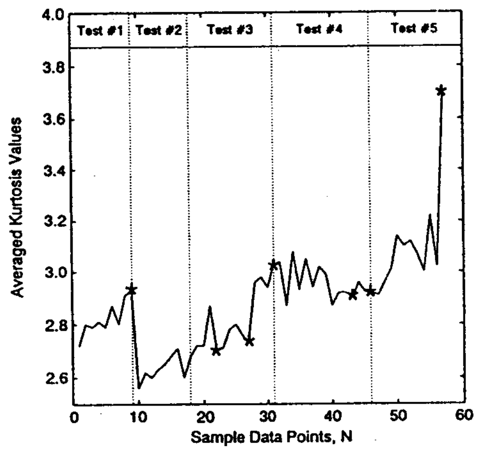

Fig. 4 Averaged kurtosis values for the five tests obtained from *Statistical Analysis*. Faults are indicated by asterisks.

particular module were not utilized in detection so as to investigate the possibility of fault detection without them. For analysis purposes, only one data record per day was used for each test. The data records were taken at the beginning of the day unless a fault was reported. When a fault was detected the record was taken right before the fault incident to ensure that the data record reflected the fault. Also, in order to reduce estimation errors, each data record was partitioned into sixteen segments and parameters were estimated for each segment and averaged over these segments. The data records as well as the parameters obtained from the above processing modules were then transferred to a personal computer for further analysis.

The parameters obtained from each module of the diagnostic analyzer are shown in Fig. 3. Note that the objective of this paper is to investigate the applicability of MVIM as a pattern classifier in fault detection of helicopter gearboxes, not to develop/verify individual diagnostic algorithms. The parameters obtained from the diagnostic analyzer comprise a wide range of parameters usually used for transmission health monitoring, but may not constitute an optimized set.

In order to show an example of the sensitivity of the obtained parameters to the occurred faults, the averaged kurtosis values of the vibration signals from the eight accelerometers are shown in Fig. 4 for the five tests. The results indicate that the kurtosis value reflects only the fault incident at the end of Test #5, and that it is not sensitive to the other six fault incidents in the other tests (marked by asterisks). The significant increase in the kurtosis value at the end of Test #5 is perhaps caused by the severity of faults at that instant (i.e., sun gear teeth spall, planet tooth spall, and top housing crack). It should be noted that while the insensitivity of individual parameters to various faults is a usual phenomenon in transmission health monitoring, it is further exacerbated here by averaging, which masks the effect of faults on individual parameters.

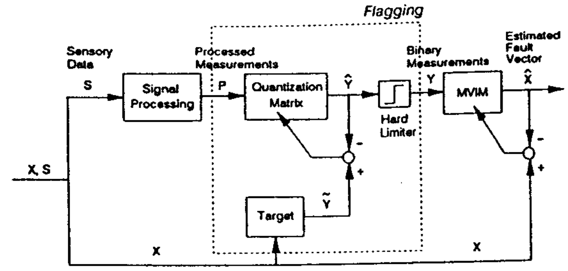

Fig. 5 Schematic diagram of adaptation in the MVIM method

4 Detection Method

The MVIM method is based on a *multi-valued influence matrix* (MVIM) which represents the signatures of various faults (Danai and Chin, 1991). Measurements in this method are monitored in-process and converted to binary numbers through *flagging*, which are posted in a vector of "flagged measurements." Flagging in this method is performed by a *quantization matrix*, and detection is performed by matching this vector of flagged measurements against the individual columns of the influence matrix (influence vectors). The influence vectors are continuously updated by a learning algorithm to improve detection. The MVIM method is explained in detail in (Danai and Chin, 1991). Its specifics insofar as detection are discussed here for completeness.

Fault signatures in the MVIM detection method are represented by the two unit-length columns $\bar{V}_j \in \Re^m$ of a multi-valued influence matrix (MVIM) $\bar{A}$ ($m \times 2$):

$$\bar{A} = [\bar{V}_1 \quad \bar{V}_2] \tag{1}$$

where m denotes the number of measurements obtained from the raw data, and $\bar{V}_1$ and $\bar{V}_2$ represent the no-fault and fault signatures, respectively. Detection is performed by obtaining $\hat{x}_1$ and $\hat{x}_2$ which represent the possibility of occurrence of the no-fault and fault cases, respectively, as

$$\hat{X} = \begin{Bmatrix} \hat{x}_1 \\ \hat{x}_2 \end{Bmatrix} = \begin{Bmatrix} \cos\alpha_1 \\ \cos\alpha_2 \end{Bmatrix} = \begin{Bmatrix} \bar{V}_1^T \bar{Y} \\ \bar{V}_2^T \bar{Y} \end{Bmatrix}. \tag{2}$$

The parameters α_1 and α_2 denote the angles between the influence vectors $\bar{V}_1$ and $\bar{V}_2$, respectively, and the vector $\bar{Y}$, which represents the normalized form of the flagged measurement vector Y. The influence matrix, $\bar{A}$, is estimated during a training session by adjusting the individual columns of the influence matrix recursively after the occurrence of each fault, or when a flag is posted in a no-fault case, so as to minimize the sum of the squared detection error (Danai and Chin, 1991).

In the MVIM detection method, flagging of measurements is performed by a *quantization matrix*. For flagging, the measurements $P \in \Re^m$ are multiplied by the columns of the *quantization matrix* Q ($m \times m$)

$$Q = [W_1 \ldots W_i \ldots W_m], \tag{3}$$

and hard-limited as

$$y_i = \begin{cases} 1 & \text{when } P^T W_i \geq H \\ 0 & \text{otherwise} \end{cases} \tag{4}$$

to produce the binary vector of flagged measurements Y (see Fig. 5). The vectors of MVIM are trained based on the flagged measurements y_i [see Eq. (4)]. Therefore, they are directly influenced by the flagging operation. In order to improve the flagging operation, the quantization matrix is adapted during a training session. Ideally, we would like the magnitude of all flagged measurements y_i to be equal to 0 for no-fault cases and 1 at fault instances. Therefore, the components of the quantization matrix are adjusted to produce such ideal flagged measurement vectors (see Fig. 5).

The quantization vectors $\mathbf{W}_i$ can be perceived as directions in m-dimensional space on which the measurements are projected. As such, the objective of training is to adjust these directions such that the projected value of the measurement vector would exceed the threshold value H for fault cases. It should be noted that the threshold value H is arbitrarily selected in the 0–1 region. While different values of the threshold H would result in different sets of $\mathbf{W}_i$, it has been found through practice that the value of H does not have a significant effect on the performance of the detection method. The projection of the measurement vector on various directions in m-dimensional space is similar to "residual transformation" in model-based methods for the purpose of obtaining "direction-fixed residuals" (e.g., see Gertler, 1991).

The *quantization matrix* uses a sample set of measurement-fault vectors to tune its parameters iteratively. For this purpose, recursive least-squares adaptation is used to minimize the sum of squared errors between the individual flagged measurements produced by the *quantization matrix* and their ideal values. This learning algorithm has the form

$$w_{ij}(\mu) = w_{ij}(\mu - 1) + l_j(\mu - 1)\left[\bar{y}_i(\mu) - \mathbf{P}^T(\mu)\mathbf{W}_i(\mu - 1)\right] \quad (5)$$

where the w_{ij} denote the components of the *quantization matrix*, μ is the iteration step, the $\bar{y}_i$ represent the ideal values of flagged measurements (i.e., $\bar{y}_i = 1$ for fault cases, and $\bar{y}_i = 0$ for no-fault cases), and the l_i denote the components of the adaptation gain vector $\mathbf{L}$, updated according to the relationship (Ljung, 1987)

$$\mathbf{L}(\mu) = \frac{\mathbf{R}(\mu - 1)\mathbf{P}^T(\mu)}{1 + \mathbf{P}(\mu)\mathbf{R}(\mu - 1)\mathbf{P}^T(\mu)} \quad (6)$$

where matrix $\mathbf{R}$ denotes the covariance matrix in least-squares estimation.

5 Detection Results

The averaged values of the nineteen parameters computed from the eight accelerometers were used as the components of the measurement vector $\mathbf{P}$ to train and test the MVIM (see Figs. 3 and 5). For scaling purposes, each parameter value was normalized with respect to the value of the parameter on the first day of each test. Note that the averaged values of the parameters were selected here to make the task of detection more difficult for MVIM as a test of its performance. For practical implementation, individual MVIMs will be trained for each accelerometer, and the final detection results will be obtained through a voting scheme based on the training speed of individual MVIMs (Chin et al., 1993).

As explained in the previous section, the MVIM method requires a set of measurements during normal operation and at fault incidents to estimate the no-fault and fault signatures. Since in the experiments the exact time of fault was not known, the time of the fault occurrence was conservatively set on the last day, or right before the fault was verified through disassembly. Similarly, no-fault cases were assumed only for the first day of each test, and after faulty components were replaced. The specification of vibration data as fault and no-fault on various days of each test are included in Table 2. For Tests #1 and #5, only the data from the last day (day 9 and day 11, respectively) were associated with a fault case, since faults in these tests were only found on the last day during routine disassembly. For Test #2, the data from all of the nine days were marked as no-fault, since no faults were detected during inspection at the end of the ninth day. For Test #3, the data from days 1, 5, and 10 were associated with a no-fault case, because they were obtained directly after faulty components were replaced on days 4, 9, and 13. For Test #4, data from days 1–8 were attributed to a no-fault case, since no faults were detected upon inspection at the end of the eighth day. For this test, the data from days 12 and 15, which were collected before faulty components were replaced, were associated with fault incidents. Note that the data from day 13, obtained directly after the replacement of the faulty component, were also associated with a no-fault case.

Table 2 Association of data from each day of the 5 tests with fault and no-fault cases. The mark "-" denotes that data from that day cannot be specified.

Day	Fault Status				
	Test #1	Test #2	Test #3	Test #4	Test #5
1	no-fault	no-fault	no-fault	no-fault	no-fault
2	-	no-fault	-	no-fault	-
3	-	no-fault	-	no-fault	-
4	-	no-fault	fault	no-fault	-
5	-	no-fault	no-fault	no-fault	-
6	-	no-fault	-	no-fault	-
7	-	no-fault	-	no-fault	-
8	-	no-fault	-	no-fault	-
9	fault	no-fault	fault	no-fault	-
10			no-fault	-	-
11			-	-	fault
12			-	fault	
13			fault	no-fault	
14				-	
15				fault	

The effectiveness of the MVIM detection method was evaluated with different training sets. For this purpose, training sets were formed based on parameters from various combinations of five tests (see Table 3). For each training case, the initial values of the MVIM (19 × 2) and the quantization matrix (19 × 19) were set to $\mathbf{O}$ and $\mathbf{I}$, respectively, the value of threshold H was set at 0.5, and training was continued until perfect detection was achieved in the training set (i.e., no false alarms or undetected faults were found in the training set). In this case, after each epoch (pass through the training set) the detection performance of MVIM was evaluated within the training set. Training was stopped when perfect detection was achieved so as to avoid overtraining (Hertz et al., 1991). The MVIM was then tested on the data from all of the five tests. The detection results produced by the MVIM for 30 different cases of training are shown in Table 3, where detection performance is characterized by the total number of false alarms and undetected faults produced during testing (denoted as Total Test Errors in Table 3).

For comparison purposes, the results from the MVIM in Table 3 are contrasted with results obtained from a feedforward neural net trained with back-propagation learning (e.g., see Hertz et al., 1991; Rumelhart et al., 1988). Note that the comparison made here is a limited one, involving only one type of neural net. However, this comparison is included so as to highlight the characteristic differences between the MVIM and neural nets insofar as the requirements for their implementation. Unlike the MVIM which has a fixed structure, the topology of neural nets needs to be selected based on their generalization ability pertaining to correct classification of patterns not included in training (Hertz et al., 1991). Neural nets with different number of hidden units, learning rate, and momentum coefficient were trained with the training sets in Table 3. The neural net which provided the best overall results had 40 hidden units, selected within a range of

Table 3 Detection results obtained from MVIM and a multi-layer neural net when trained with different data sets

Case #	Training Data Sets	Diagnostic Method	Undetected Faults	False Alarms	Total Test Errors
1	1	Neural Net	4	0	4
		MVIM	1	3	4
2	3	Neural Net	1	3	4
		MVIM	1	1	2
3	4	Neural Net	5	1	6
		MVIM	2	1	3
4	5	Neural Net	1	2	3
		MVIM	3	2	5
5	1,2	Neural Net	4	0	4
		MVIM	2	2	4
6	1,3	Neural Net	1	2	3
		MVIM	2	0	2
7	1,4	Neural Net	1	1	2
		MVIM	1	1	2
8	1,5	Neural Net	1	2	3
		MVIM	1	2	3
9	2,3	Neural Net	1	1	2
		MVIM	1	1	2
10	2,4	Neural Net	4	2	6
		MVIM	3	1	4
11	2,5	Neural Net	3	2	5
		MVIM	3	2	5
12	3,4	Neural Net	2	2	4
		MVIM	0	0	0
13	3,5	Neural Net	0	3	3
		MVIM	1	0	1
14	4,5	Neural Net	3	0	3
		MVIM	1	1	2
15	1,2,3	Neural Net	1	2	3
		MVIM	2	0	2
16	1,2,4	Neural Net	2	1	3
		MVIM	2	1	3
17	1,2,5	Neural Net	1	2	3
		MVIM	1	2	3
18	1,3,4	Neural Net	1	0	1
		MVIM	0	0	0
19	1,3,5	Neural Net	0	3	3
		MVIM	2	0	2
20	1,4,5	Neural Net	1	1	2
		MVIM	1	1	2
21	2,3,4	Neural Net	2	0	2
		MVIM	0	0	0
22	2,3,5	Neural Net	1	2	3
		MVIM	1	0	1
23	2,4,5	Neural Net	3	1	4
		MVIM	1	1	2
24	3,4,5	Neural Net	2	0	2
		MVIM	0	0	0
25	1,2,3,4	Neural Net	2	0	2
		MVIM	0	0	0
26	1,2,3,5	Neural Net	2	1	3
		MVIM	1	0	1
27	1,2,4,5	Neural Net	1	1	2
		MVIM	1	1	2
28	1,3,4,5	Neural Net	1	0	1
		MVIM	0	0	0
29	2,3,4,5	Neural Net	2	0	2
		MVIM	0	0	0
30	1,2,3,4,5	Neural Net	1	0	1
		MVIM	0	0	0

30 to 50 hidden units, and the learning rate and momentum coefficient of 0.2 and 0.8, respectively, selected within a range of 0 to 1.

The results in Table 3 indicate that the MVIM was able to provide perfect detection when faults were fully represented by the training sets (i.e., Cases #18, #21, #24, #25, #28, #29, and #30), and that it produced better results than the neural net in most of the cases. Specifically, the MVIM produced better results in nineteen of the test cases, produced identical results in ten cases, and was outperformed in only one case. Upon a casual inspection of the training sets with which MVIM produced perfect detection, it is observed that Tests #3 and #4 were included in all of them. This implies that the MVIM needed the parameters from these two tests to establish an effective pair of signatures for no-fault and fault cases, and that its performance was not adversely affected when data from additional tests were included in training. Without Test #3, the MVIM produced one undetected fault and one false alarm (Case #27), and without Test #4 it produced one undetected fault (Case #28). The neural net was observed to be more sensitive to its training environment. For example, the neural net produced only one undetected fault for Case #18, when trained with Tests #1, #3, and #4, whereas it produced two undetected faults when Test #2 was also included in training (Case #25). The net could not provide accurate detection even when trained with all of the five tests (Case #30).

None of the parameters used in this study reliably reflect the faults which occurred in the experiments. However, this is not an unusual phenomenon in transmission health monitoring. One approach towards this problem is to continue searching for the "ideal" parameter. The other approach, which is demonstrated here, is to integrate the information available in the existing parameters through pattern classification. In the pattern classification domain, the MVIM method is shown to have two important features: (*1*) it has a fixed structure, which eliminates the need for trial and error testing, and (*2*) it has a robust performance.

6 Measurement Selection

The MVIM method may also be used to assess the significance of individual parameters for detection. The underlying basis is the hypothesis that "important measurements" (i.e., those which reflect the faults more effectively) facilitate training, so their presence (absence) decreases (increases) the number of training epochs required. In other words, when an "important measurement" is discarded from the training set, training should become more difficult and time-consuming, because the no-fault and fault signatures will have to be characterized by the remaining measurements.

In order to test the above hypothesis, a training set which produced perfect detection results was selected. Among the various training sets in Table 3 satisfying this condition, Case #12 which contained the smallest training set (i.e., Tests #3 and #4) was selected. Individual parameters were then discarded one at a time from this training set and MVIM was retrained with the remaining parameters. The number of training epochs required for each reduced set is shown in Table 4, with the discarded parameters imposing higher than 9 epochs (obtained for the full set) marked by a plus sign.

Based on the results in Table 4, the elimination of Parameters #3 (crest factor), #11 (TM1-P), #12 (CEP(1911)), #13 (CEP(572)), #14 (TON(1911)), #15 (TON(572)), #16 (BE), and #17 (BKV) from the training set adversely affected training. This implies that these eight parameters are particularly important in characterizing the signatures for the no-fault and fault cases, and that Parameter #12, whose elimination jeopardized training, is critical. By the same analogy, the results in Table 4 indicate that discarding Parameters #7 and #18 may be even beneficial to training of MVIM.

In order to validate the above findings, various combinations of parameters from Tests #3 and #4 were grouped into subsets. Training started with the smallest possible subset which included only two parameters. As the MVIM did not converge with this subset, the subset was expanded further until successful training was obtained. The first subset that resulted in perfect training for the MVIM and perfect detection results for all the tests was one with twelve parameters, of which eight parameters were those identified as "important" in Table 4 (i.e., Parameters #3, #11, #12, #13, #14, #15, #16, and #17). In fact, through further analyses it was found that the smallest subset of parameters that provided perfect training for the MVIM consisted of these eight pa-

Table 4 The effect of discarded parameters on training time and test results. The particular sets that required a longer training time than the full set are marked by "+". The "*" denotes that full detection within the training set was never achieved.

Case # 12 (Test # 3 and #4)			
Parameter Discarded	Number of Training Epochs	Undetected Faults	False Alarms
None	9	0	0
#1	9	0	0
#2	9	0	0
#3+	25	0	0
#4	9	0	0
#5	9	0	0
#6	9	0	0
#7	8	0	0
#8	9	0	0
#9	9	0	0
#10	9	0	0
#11+	10	0	0
#12+	100*	0	6
#13+	11	0	0
#14+	10	0	0
#15+	37	0	0
#16+	10	0	0
#17+	22	0	2
#18	8	0	0
#19	9	0	0

rameters, and that discarding or replacing any of these eight parameters resulted in a non-trainable situation. Addition of more parameters to this subset did not improve the training time.

The measurement selection approach described above can only be performed with a fixed-structure classifier like MVIM. In multi-layer neutral nets the amount of training is a function of the net topology as well as its training set. Since for a reduced training set the optimal topology of the neutral net may differ, the number of training epochs is not representative of the quality of the training set. The ability to select the "important measurements" is particularly significant in cases such as helicopter power train diagnosis, where the computation of all the parameters may not be feasible in real-time.

7 Conclusion

Fault detection of helicopter power transmissions through pattern classification is demonstrated. For this purpose, vibration data collected during normal operation and at fault instances from an OH-58A main rotor transmission is used. The detection method is the Multi-Valued Influence Matrix (MVIM) method which constructs the no-fault and fault signature based on vibration data reflecting the effect of various faults. Implementation results indicate that the MVIM method provides accurate detection when the full range of fault effects is represented in the vibration data, and that it has a more robust performance than the feedforward neural net it is compared with. The MVIM method is also used to assess the significance of individual measurements. The results presented indicate that the MVIM method is a viable tool for sensor integration and selection, and that it should be considered for in-flight diagnostics. In that context, the vibration data will need to be processed in real-time and fed to the MVIM, which has been trained *a-priori* to represent the no-fault and fault signatures.

Acknowledgments

The authors would like to express their gratitude to Sikorsky Aircraft Company for its continued support of this project and NASA for providing the experimental data. This work was supported in part by the National Science Foundation (Grants No. DDM-9015644 and MSS-9102149).

References

Astridge, D. G., 1986, "Vibration Health Monitoring of the Westland 30 Helicopter Transmission—Development and Service Experience," *Mechanical Failure Prevention Group 41th Meeting*, Oct., pp. 200–215.

Braun, S., 1986, *Mechanical Signature Analysis—Theory and Applications*, Academic Press, New York, NY.

Cempel, C., 1988, "Vibroacoustical Diagnostics of Machinery: An Outline," *Mechanical Systems and Signal Processing*, Vol. 2, No. 2, pp. 135–151.

Chin, H., and Danai, K., 1991, "Fault Diagnosis of Helicopter Power Trains," *Proc. of the 17th Annual NSF Grantees Conference in Design and Manufacturing Systems Research*, Austin, TX, Jan., pp. 787–790.

Chin, H., Danai, K., and Lewicki, D. G., 1993, "Pattern Classifier for Fault Diagnosis of Helicopter Gearboxes," IFAC *J. of Control Engineering Practice*, Vol. 1, No. 5, pp. 771–778.

Collier-March, M. E., and Astridge, D. G., 1985, "Operational Experience with the Advanced Transmission Health Monitoring Techniques on the Westland 30 Helicopter," *11th European Rotorcraft Forum*, p. 43.

Danai, K., and Chin, H., 1991, "Fault Diagnosis with Process Uncertainty," ASME *Journal of Dynamic Systems, Measurement and Control*, Vol. 113, No. 3, Sept., pp. 339–343.

Dimarogonas, A., and Haddad, S. D., 1992, "Machinery Vibrations: Monitoring and Diagnosis," Chapter 14 of *Vibration for Engineers*, Prentice-Hall, Inc., Englewood Cliffs, NJ.

Gertler, J. J., 1991, "Analytical Redundancy Methods in Fault Detection and Isolation," *Proc. of IFAC SAFEPROCESS Symposium*, Baden-Baden, Germany.

Hertz, J., Krogh, A., and Palmer, R. G., 1991, *Introduction to the Theory of Neural Computation*, Addison-Wesley, Redwood City, CA.

Kaufman, A. B., 1975, "Measure Machinery Vibration—It Can Help You Anticipate and Prevent Failure," *Instruments & Control Systems*, Feb., pp. 59–62.

Lewicki, D. G., Decker, H. J., and Shimski, J. T., 1992, "Full-Scale Transmission Testing to Evaluate Advanced Lubricants," Technical Report, NASA TM-105668, AVSCOM TR-91-C-035.

Ljung, L., 1987, *System Identification: Theory for the User*, Prentice-Hall, Inc., Englewood Cliffs, NJ.

Mertaugh, L. J., 1986, "Evaluation of Vibration Analysis Techniques for the Detection of Gear and Bearing Faults in Helicopter Gearboxes," *Mechanical Failure Prevention Group 41th Meeting*, Oct., pp. 28–30.

Pratt, J. L., 1986, "Engine and Transmission Monitoring—A Summary of Promising Approaches," *Mechanical Failure Prevention Group 41th Meeting*, Oct., pp. 229–236.

Rumelhart, D. E., Hinton, G. E., and Williams, R. J., 1988, "Learning Error Representation by Error Propagation," Rumelhart, D. E. and McClelland, J. L., eds., *Parallel Distributed Processing—Explorations in the Microstructure of Cognition, Volume 1: Foundations*, The MIT Press, Cambridge, MA.

Stewart Hughes Limited, 1986, *MSDA User's Guide*, Southampton, UK.